Development of the Los Alamos solid-state optical refrigerator

Bradley C. Edwards
Mail Stop D436, Los Alamos National Laboratory, Los Alamos, New Mexico 87545

Melvin I. Buchwald
224 La Cruz Road, Santa Fe, New Mexico 87501

Richard I. Epstein
Mail Stop D436, Los Alamos National Laboratory, Los Alamos, New Mexico 87545

(Received 28 January 1997; accepted for publication 17 February 1998)

Laser-induced cooling of a solid by net anti-Stokes fluorescence, first experimentally demonstrated in 1995, can be the basis of a new type of cryocooler, an *optical refrigerator*. This article describes the physics and design issues of a practical optical refrigerator for operation at 77 K. In particular, the Los Alamos Solid-State Optical Refrigerator (LASSOR) which we are developing would have an operating efficiency comparable to commercial small cryocoolers, be completely vibration-free and operate for years without maintenance. [S0034-6748(98)02205-9]

I. INTRODUCTION

Recent laboratory measurements demonstrated laser-induced optical refrigeration in both solids[1–3] and liquids.[4,5] It is possible to pump a solid with monochromatic radiation such that the resulting fluorescence has an average photon energy higher than that of the pump radiation. If the fluorescent quantum efficiency is high enough, the solid will cool. The first experimental demonstration of cooling, using an ytterbium-doped fluoride glass, operated with a 2% cooling efficiency.[1]

The design studies described in this article show that this optical refrigeration can be used to produce a practical first-generation Los Alamos Solid-State Optical Refrigerator (LASSOR) which, using currently available solid-state technology, would

(i) produce no vibrations, and
(ii) neither generate nor be affected by electromagnetic interference.

We estimate that this device would

(i) cool to $\leqslant$77 K from room temperature,
(ii) convert $\sim$0.5% of the applied electric power to heat lift at 77 K,
(iii) weigh less than 2 kg per W of cooling power, and
(iv) have a continuous operating lifetime of years.

II. FIRST-GENERATION LASSOR

A. Overall design

Figure 1 illustrates one design for a LASSOR that would produce 0.5 W of cooling at 77 K with efficiency comparable to that of small commercial mechanical cryocoolers. This design is based on a cooling element of Yb^{3+}-doped ZBLANP (a heavy metal fluoride glass containing zirconium, barium, lanthanum, aluminum, sodium, and lead).

This design employs recently developed high-power diode lasers that efficiently produce pump radiation at the required wavelength. An optical fiber carrying the pump radiation passes through the wall of the cryocooler vacuum chamber to a cylindrical block cooling element. Dielectric mirrors for reflecting the pump radiation are deposited on both ends of the cooling element. The pump radiation enters the cooling element through a small hole in one of the mirrors and is largely beamed along the axis of the cylinder. This light is repeatedly reflected between the dielectric mirrors and from the sides of the glass cylinder (by total internal reflection) until it is entirely absorbed by Yb^{3+} ions. The ions subsequently fluoresce isotropically in a broad spectral band. Most of the fluorescent radiation escapes from the cooling element and is absorbed by the warm walls of the cooling chamber. The object to be cooled (the cold finger in Fig. 1) is mounted on one of the mirrors of the cooling element and is thus shielded from the pump and fluorescent radiation.

The design of each component in a LASSOR requires tradeoffs and optimization. In the following sections we examine some of these considerations and their effects on the performance of the cooler.

1. Cooling element material:

The cooling material must exhibit anti-Stokes fluorescence with a high quantum efficiency. Additionally, parasitic processes must not convert the pump radiation to heat at a rate that competes with the expected cooling. These requirements are well satisfied by ultrapure ZBLANP:Yb^{3+}.

The Yb^{3+} ion has a simple energy level structure consisting of a ground-state and a single excited-state manifold at $\sim$10 000 cm^{-1} (see inset of Fig. 2). The room temperature fluorescence and absorption spectra of ZBLANP:Yb^{3+} shown in Fig. 2 indicate that if the Yb deexcites by photon emission with $\sim$100% quantum efficiency optical refrigeration is achievable with this material. Each fluorescent photon

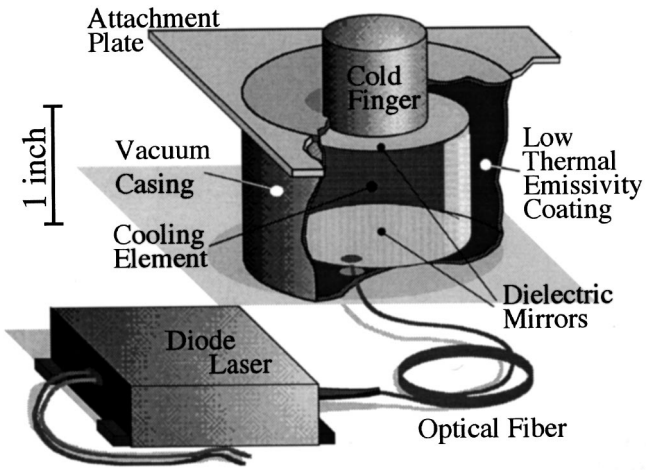

FIG. 1. A possible LASSOR design.

carries off, on average, thermal energy equal to the difference between the pump photon and the mean energy of the fluorescent photons. Since the mean energy of the fluorescent photons corresponds to a wavelength of $\lambda_F = 995$ nm, if the ion is pumped with radiation at wavelengths greater than 995 nm, energy is removed from the system, and the glass cools. When there are no parasitic heat sources, the cooling power, P_{cool}, is proportional to the absorbed pump power, P_{abs}, and to the average difference in the photon energies of the pump and fluorescent radiation. In terms of wavelength λ of the pump radiation, the cooling power P_{cool} is

$$P_{\text{cool}}(\lambda) = P_{\text{abs}}(\lambda)(\lambda - \lambda_F)/\lambda_F \equiv \eta P_{\text{abs}}. \quad (1)$$

Since the cooling is, at most, several percent efficient, a small fraction of the excitations decaying by heat-producing processes will overwhelm the optical refrigeration. In pure ZBLANP:Yb^{3+} this is not a problem. The radiative lifetime of the upper manifold is ~2 ms, whereas the nonradiative decay lifetime, which involves the simultaneous emission of more than 15 phonons, is inferred from an ''energy gap law'' to be much greater than a year![6]

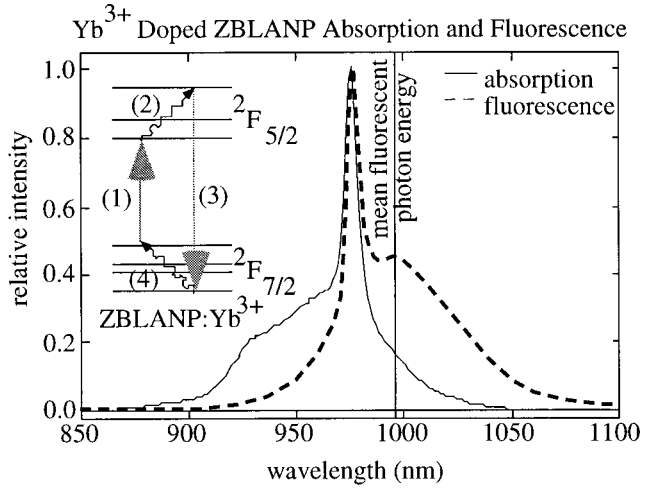

FIG. 2. Main plot—Absorption coefficient (solid curve) and fluorescence spectrum (dashed curve) at room temperature for ZBLANP:Yb^{3+} glass. The wavelength corresponding to the mean energy of the fluorescent photons, λ_F is indicated by a vertical line at 995 nm. Inset plot—The schematic energy level structure of ZBLANP:Yb^{3+}; the splittings within each group have been exaggerated for clarity. The arrows denote a cooling cycle: (1) laser pumping, (2) phonon absorption, (3) radiative decay, and (4) additional phonon absorption.

If multiphonon emission were the only nonradiative process, essentially all of the decays would occur radiatively. Nonradiative transitions can be a problem, however, when contaminants are present. A Yb^{3+} excitation can be quenched by transferring its energy to a nearby contaminant ion such as Dy^{3+}, Sm^{3+}, Fe^{3+}, etc. These impurity ions would quickly produce heat through nonradiative decays. The severity of this problem is amplified by spatial migration processes in which excitations move among neighboring Yb^{3+} ions increasing the chance that the excitations will find a quenching impurity.

The absorption and fluorescence spectra vary with temperature and change the performance of the system.[7] We have measured the absorption and fluorescence spectra of ZBLANP:Yb^{3+} over a wide temperature range and have fit the energy levels, widths, and probabilities for transitions between each of the states. Our model assumes that the relative energy level populations among the states within each manifold (lower and upper) follow Boltzmann distributions for the sample temperature. (The relative populations of the two manifolds, however, depend on the laser pumping rate and is far from thermal equilibrium).

In Fig. 3 we show the measured fluorescence and absorption spectra for ZBLANP:Yb^{3+} at temperatures between 10 and 300 K. Along with the measured spectra are our fits as discussed above. A single set of parameters describing the widths, transition strengths, and energy levels are used for all of the fits. The change with temperature is due to the population change as descibed by the Boltzmann distribution. Variations in the width, which have been recently measured,[8] have not been included in this model. The temperature dependent characteristics of the measured data are reproduced sufficiently well by our model to predict the performance of a cryocooler. As the temperature decreases, the mean fluorescent wavelength shifts to longer values and the long-wavelength absorption diminishes. Both effects decrease the optical refrigeration effect at low temperatures.

2. Cooling element pumping

To realize the greatest cooling efficiency the pump radiation should have the longest possible wavelength consistent with being absorbed in the cooling material [see Eq. (1)]. Since the absorptivity decreases at long wavelength (see Fig. 2), satisfying these two conditions requires that the radiation be trapped in the cooling element until it is absorbed. Additionally, the system must allow for the fluorescence to escape with little reabsorption.

In the first-generation LASSOR design dielectric mirrors on the ends of the cooling element trap the pump radiation. The laser radiation enters the cooling element in a narrow cone aligned with the axis of the cylinder. The divergence is sufficiently low that the light is almost perfectly reflected from the dielectric mirrors at the ends or by total internal reflection from the sides of the cooling element. The trapping efficiency is determined by the quality of the glass, mirror

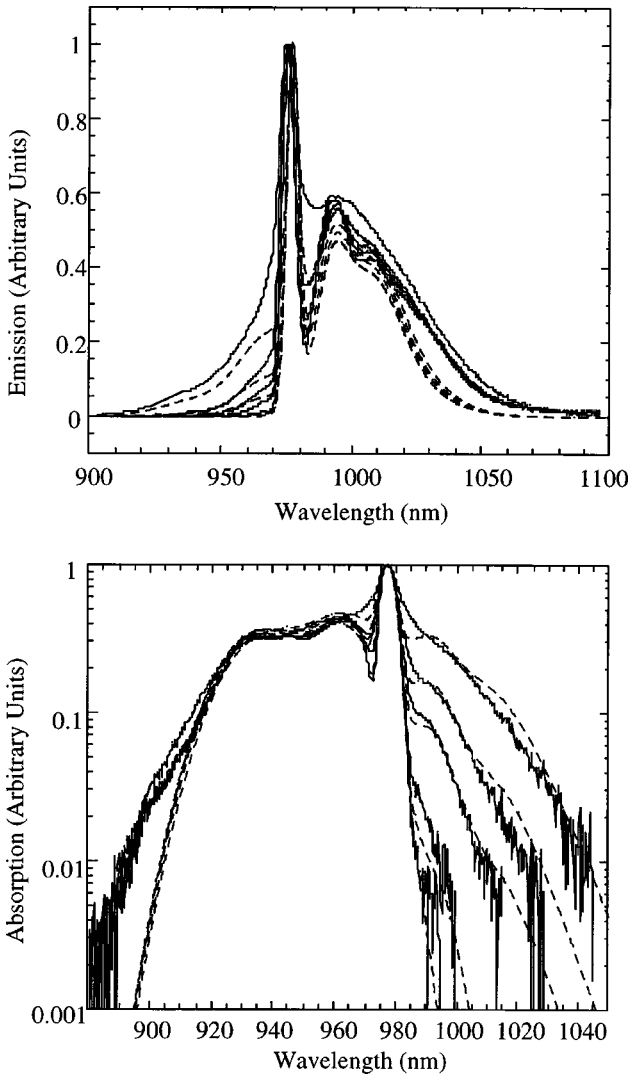

FIG. 3. The upper plot shows the measured (solid line) and model fit (dashed line) emission spectra for ZBLANP:Yb^{3+} glass at 10, 50, 100, 150, and 300 K. The lower plot shows the absorption data (solid line) and model fit (dashed line) for the same temperatures. All of the spectra have been normalized to the main peak for clarity. In the model we fit the transition strengths and the energy, and width of the levels in all of the spectra simultaneously. Gaussian line shapes were used instead of a Voigt profile. The population of the energy levels are based on a Boltzmann distribution. The model fits accurately reproduce the mean fluorescence and the absorption tails at wavelengths longer than 1000 nm. The deviations between the model and data are largely attributable to our neglect of the Voigt profile and the temperature dependence of the linewidths. These discrepancies do not significantly affect the performance estimate.

construction, and the ratio of the mirror area to the area of the entrance hole through which the pump light enters. Several practical considerations determine the attainable trapping efficiency:

(i) Commercially available dielectric mirrors have reflectivities $R>99.97\%$ for angles within 30° of normal. Most of the remaining light leaks through the mirror. Only about 1% of the unreflected light is absorbed in the mirror and converted into heat.

(ii) Because trapped light escapes through the entrance hole, the light leakage per reflection is equal to the ratio of the area of the hole to the total area of both mirrors. In the current design, which uses a 0.4 mm diam hole and 30 mm diam mirror, the leakage per reflection is $<10^{-3}$.

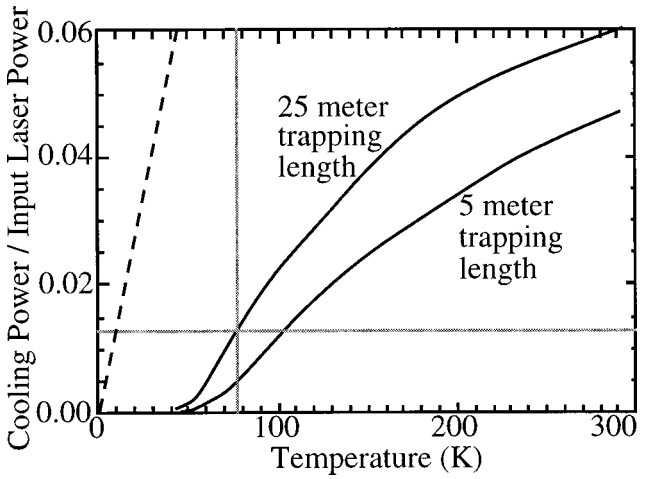

FIG. 4. Calculated cooling efficiency vs temperature for a 5 and 25 m pathlength of 2% Yb^{3+}-doped ZBLANP. The dashed line gives the thermodynamic limit on the cooling efficiency for the Yb-based optical refrigerator (see the Appendix).

With these mirror and hole characteristics, assuming that the cylinder is uniformly filled, light pumped in through the entrance hole will be trapped for 2000 passes on the average. This corresponds to a 50 m trapping length in a 2.5 cm long cylinder. Assuming that other losses will affect the trapping ability of this design we have based our calculations on trapping lengths of 5 and 25 m. Figure 4 shows that with these trapping path lengths useful cooling efficiency can be achieved in a ZBLANP:Yb^{3+} to below 70 K. With a 25 m pathlength, light to cooling power conversion efficiencies of 1.3% should be attainable at liquid nitrogen temperature (77 K). These efficiencies are well below the thermodynamic limit for a Yb-based optical refrigerator of the size and power considered (see the Appendix).

In the situation presented here, with isotropic fluorescent radiation emitted from a uniformly pumped cylinder, the amount of emitted radiation that escapes from the cylinder with one or fewer internal reflections can be calculated using simple ray-tracing methods. The fraction escaping from the ends of the cylinder will be a cone with a half angle less than the internal reflection angle for all emitted radiation. The light escaping out the sides of the cylinder must be calculated by integrating them over each axially symmetric ring of emitting glass. In an ideal ZBLANP cylinder with equal length and diameter dimensions 78% of the fluorescence escapes with less than two internal reflection from a surface. When the cooling element has perfect broadband mirrors on both ends, 48% of the light escapes with less than two internal reflections. Most of the fluorescence that is trapped by internal reflections is reabsorbed and then reemitted by the Yb^{+3} ions.

3. Radiation control

An important part of the design of an effective optical refrigerator is controlling the flows of both fluorescent radia-

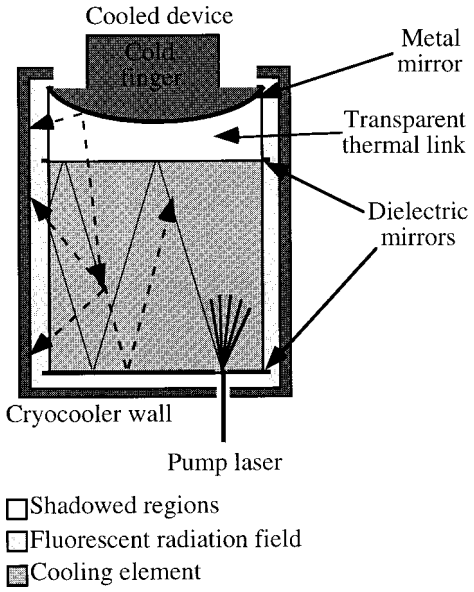

FIG. 5. Cooling element and cold finger design. The input laser light is shown as solid lines and the fluorescence as dashed. Light gray areas show where the fluorescent radiation field is most intense. White regions are regions in the shadow of the dielectric mirrors. These shadowed regions are not completely free of fluorescent radiation due to leakage through the dielectric mirrors. An additional metal mirror and baffles prevent any fluorescent radiation from reaching the objects to be cooled.

tion and thermal radiation between the cooling element and the walls. To decrease the heat load on the cooling element from the thermal radiation of the walls, low emissivity coatings can be used on the walls that will reduce the thermal load by a factor of >10 relative to that of a blackbody surface.[9] These same surfaces can effectively absorb $>95\%$ of the 1 μm fluorescent radiation in our design and convert it to heat. These coating materials function by having a surface that is smooth on the scale of thermal radiation (10 μm) but extremely rough on the scale of the fluorescence radiation (1 μm). The wall temperature can be limited by several methods including conduction to a thermal sink. The fluorescence that is reflected back by these coatings will add only about 5% to the outgoing fluorescent flux density in the cavity. The light reflected from the walls cannot become trapped in the glass element because of its incident angle, only a small fraction ($<10\%$) of this light can be reabsorbed in our design.

The fluorescent radiation field has to be carefully considered in designing the connections between the cooling element and the device being cooled. The *cold finger* must be thermally connected to the cooling element, yet shielded from exposure to the fluorescent radiation. Figure 5 shows one design for the cold finger connection. A transparent material that is a good thermal conductor is attached to the back of the mirror opposite the input hole. A curved metal mirror affixed to this conductor creates a shadowed region by blocking both radiation leaking through the dielectric mirror and stray fluorescent radiation. The cold finger connected to the back of the mirror is located inside the umbra of this shadow.

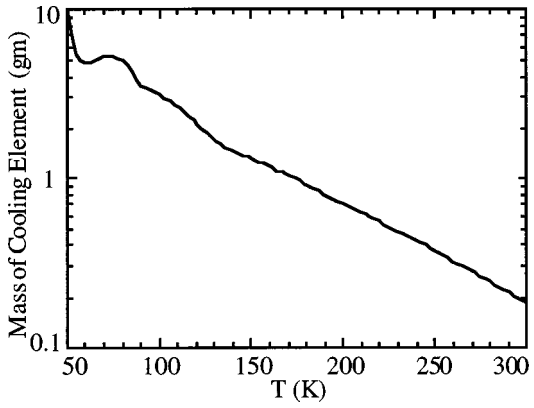

FIG. 6. The minimum mass of the cooling element of a 0.5 W, ZBLANP:Yb^{3+} optical refrigerator.

4. Cooler power

The maximum energy an optical refrigerator could extract depends on the mass of the cooling element, the Yb^{3+} concentration, and the operating temperature. The cooling power is

$$P_{\text{cool}} = \eta P_{\text{abs}} \approx \eta h \nu_F N(\text{Yb}^*)/t_{\text{rad}}, \tag{2}$$

where $h\nu_F = hc/\lambda_F$ is the mean energy of the fluorescent photons, N(Yb*) is the total number of excited ytterbium ions in the cooling element, and t_{rad} is the radiative decay time scale of the excited ytterbium ions. Radiative pumping cannot raise the occupation number of an energy level in the excited manifold to a value greater than that of the of the pumped level in the ground state manifold. If the energy of the pumped level in the ground state manifold is E_a, the maximum number of excited ytterbium ions $N(\text{Yb}^*)_{\max}$ is

$$N(\text{Yb}^*)_{\max} \propto N(\text{Yb}) \exp(-E_a/kT). \tag{3}$$

Here $N(\text{Yb})$, the total number of ytterbium ions, is proportional to the product of the Yb concentration and the mass of the cooling element, and k is the Boltzmann constant.

As an illustration, Fig. 6 gives the required mass of the cooling element for a 0.5 W unit with 2 wt % of Yb^{3+}. For this curve we estimate E_a to be the energy difference between the bottoms of the excited and ground state manifolds (corresponding to the 975 nm peak in the spectrum of Fig. 1) and the pump radiation at $\lambda = \lambda_F(1+\eta)$ with the efficiency given by the upper solid curve of Fig. 4. For the 0.5 W optical refrigerator to operate at 77 K, the cooler element would have to be at least 6 g; this corresponds to a cylindrical element with both a height and a diameter of 1.3 cm.

5. Pump laser

A LASSOR requires a radiation source that is compact, efficient, reliable, and rugged and has the needed power, wavelength, and divergence characteristics. Fortunately, recently developed high-power diode lasers operate around 1.02 μm, the optimal operating wavelength, and can supply the needed 50 W of input power. The efficiency (dc electrical to optical power) of these types of lasers can be as high as 66%.[10]

Available high-power diode lasers have lifetimes of 10 000 h. Diodes lasers being developed may have much longer lives.[11] Until these lasers are available, optical refrigerators could employ redundant lasers to assure reliability and long operation.

6. Future developmental work

Combining the individual components discused above into a working practical system will require considerable optimization. A proof-of-principle cryocooler development effort is underway at Los Alamos National Laboratory to demonstrate the basic principle of optical cooling and provide experience for optimizing a practical system. Following the proof-of-principle work an engineering model for a practical cryocooler can be developed. Three parameters critical for possible applications of this technology are: (1) the mass of the system, (2) the operating life, and (3) the overall efficiency.

The mass of a practical LASSOR can be estimated from the individual components: (1) for 0.5 W of cooling power the cooling element must be >10 g, (2) an outer vacuum wall thick enough to remove waste heat could be up to 350 g, (3) laser diodes with heat sinks would be 200 g, and (4) a simple dc to dc converter with housing would be 300 g. The thermal links and sinks would be diamond coated aluminum or copper. A realistic estimate of the mass for a 0.5 W LASSOR is about 1 kg.

Several factors could determine the lifetime of a LASSOR. The laser diodes are the only component of the LASSOR with a known failure mode (10 000 h lifetimes and increasing). If the LASSOR is used for space applications, radiation damage of the glass element needs to be considered although studies suggest that this will not be a serious problem.[12] A first-generation LASSOR could operate continuously for several years if improved or redundant diode lasers are used.

An estimate of the overall efficiency of a first-generation or practical system can be calculated based on current technology: (1) the optimal cooling efficiency of the cooling element is predicted to be 1.3% at 77 K, (2) high-performance fiber coupling efficiency can be 95%, (3) three fiber couplings may be required for a practical device, (4) laser diodes at the power and wavelength required can be 50% efficient, and (5) thermal radiation load can be minimized through the use of designed coatings on the walls. From these numbers a first-generation LASSOR could have a 0.5% ratio of heat lift to dc electrical power.

In summary, our work illustrates the possibility of development of a new type of cryocooler that is fully solid-state and has good mass, efficiency, vibration, lifetime, and ruggedness characteristics. Each of the components are commercially available and the scientific principles have been demonstrated. Models of the principles and operations of this system show the possibility of operation at temperatures below 77 K with a single-stage unit. Continued engineering and basic research is required to optimize the proposed system.

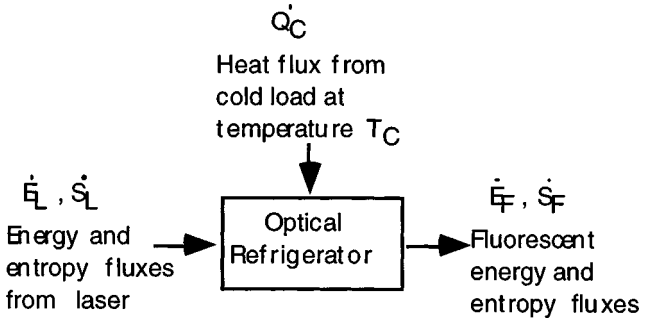

FIG. 7. The energy and entropy fluxes for optical refrigeration.

ACKNOWLEDGMENTS

The authors thank Timothy Pfafman and W. R. Scarlett for helpful discussions and comments. This work was carried out under the auspices of the U.S. Department of Energy and was supported in part by IGPP at LANL.

APPENDIX

1. Thermodynamics of optical refrigeration

The second law of thermodynamics gives the maximum efficiency of an optical refrigerator if one includes the energy and entropy fluxes of the pump radiation and the fluorescent radiation as well as those from the heat load.[13,14] As indicated in Fig. 7, energy and entropy are removed from the laser pump radiation at rates $\dot{E}_L$ and $\dot{S}_L$, respectively, and are added to the fluorescent radiation field at rates $\dot{E}_F$ and $\dot{S}_F$. The cold load at temperature T_C loses thermal energy at a rate $\dot{Q}_C$ and thus loses entropy at a rate $\dot{Q}_C/T_C$. An optical refrigerator operating in steady state does not change its internal energy or entropy. Conservation of energy gives

$$\dot{E}_L+\dot{Q}_C=\dot{E}_F \tag{A1}$$

and the second law of thermodynamics states that the total entropy does not decrease, i.e.,

$$\dot{S}_F-\dot{S}_L-\frac{\dot{Q}_C}{T_C}\geqslant 0. \tag{A2}$$

In terms of the laser and fluorescence *flux temperatures*, $T_L \equiv \dot{E}_L/\dot{S}_L$ and $T_F \equiv \dot{E}_F/\dot{S}_F$, Eqs. (A1) and (A2) can be rewritten to give

$$\dot{E}_L\left(\frac{T_F}{T_L}\right)+\dot{Q}_C\left(\frac{T_F}{T_C}\right)\leqslant \dot{E}_F=\dot{E}_L+\dot{Q}_C. \tag{A3}$$

The refrigerator cooling efficiency η for conversion of light to heat lift is thus

$$\eta=\frac{\dot{Q}_C}{\dot{E}_L}\leqslant\frac{1-(T_F/T_L)}{(T_F/T_C)-1}. \tag{A4}$$

For the conditions relevant to an optical refrigerator, the flux temperature of the laser radiation is much higher than that for the fluorescence which, in turn, is higher than the load temperature; i.e., $T_L \gg T_F > T_C$. For these limits the constraint on the efficiency reduces to

$$\eta \leqslant \frac{T_C}{T_F - T_C}. \tag{A5}$$

This form is similar to Carnot efficiency, except that the fluorescence flux temperature T_F replaces the usual temperature of the hot thermal reservoir. To evaluate T_F, we examine the entropy and energy carried by the fluorescent photons. The entropy density of photons is

$$\rho_S = k \int [(1+n)\ln(1+n) - n\ \ln(n)]\rho_\gamma\ d\epsilon\ d\Omega, \tag{A6}$$

where k is Boltzmann's constant, $\rho_\gamma = 2\epsilon^2/h^3c^3$ is the density of photon of states per unit energy ϵ and solid angle Ω, and $n\ (\epsilon,\Omega)$ is the occupation number per state. Two sources contribute to the occupation numbers, ambient thermal photons and fluorescent photons from the refrigerator; i.e.,

$$n(\epsilon,\Omega) = n_A(\epsilon) + n_F(\epsilon,\Omega). \tag{A7}$$

The contribution of the ambient radiation at temperature T_A is

$$n_A(\epsilon) = [\exp(\epsilon/kT_A) - 1]^{-1}. \tag{A8}$$

The *excess* entropy density due to the addition of the fluorescent emission is

$$\rho_S^F = k \int \{[(1+n)\ln(1+n) - n\ \ln(n)] - [(1+n_A)\ln(1+n_A) - n_A\ \ln(n_A)]\}\rho_\gamma\ d\epsilon\ d\Omega, \tag{A9}$$

and the *excess* energy density due to the fluorescent emission is

$$\rho_E^F = \int \epsilon n_F \rho_\gamma\ d\epsilon\ d\Omega. \tag{A10}$$

Since the entropy and energy fluxes of the fluorescence are proportional to the excess entropy and energy densities, the fluorescent temperature is

$$T_F \cong \frac{\rho_E^F}{\rho_S^F}. \tag{A11}$$

We now apply these results to the first-generation LASSOR. To achieved 0.5 W of cooling power, this device uses about 40 W of radiation. A cylindrical cooling element with height and diameter of 3 cm emits an average fluorescent flux of $\sim 0.9\ \mathrm{W/cm^2}$. To estimate the energy and entropy fluxes, we take the fluorescent radiation to be uniform over the surface area of the cooling element and isotropic in the outgoing hemisphere. The occupation number follows the fluorescent spectrum of Fig. 2 and has a peak value of $n_{F,\max} \sim 5 \times 10^{-8}$. For $T_A = 290$ K, the ambient radiation contribution is $n_A \sim 10^{-22}$ and can be neglected. (In practical optical refrigerators the effects of the ambient radiation are negligible. The ambient radiation needs to be included in the formalism only to ensure that the Carnot limit is never violated; i.e., T_F must always exceed T_A, even in the limit of vanishingly small fluorescent flux.)

Using the above values, Eq. (A11) gives a fluorescent temperature of $T_F = 773$ K. The thermodynamic limit on the efficiency, given by Eq. (A5) is shown in Fig. 4. The performance of the first-generation LASSOR will be at least a factor of six below the thermodynamic limit.

[1] R. I. Epstein, M. I. Buchwald, B. C. Edwards, T. R. Gosnell, and C. E. Mungan, Nature (London) **377**, 500 (1995).
[2] C. E. Mungan, M. I. Buchwald, B. C. Edwards, R. I. Epstein, and T. R. Gosnell, Phys. Rev. Lett. **78**, 1030 (1997).
[3] C. E. Mungan, M. I. Buchwald, B. C. Edwards, R. I. Epstein, and T. R. Gosnell, Appl. Phys. Lett. **71**, 1458 (1997).
[4] J. L. Clark and G. Rumbles, Phys. Rev. Lett. **76**, 2037 (1996).
[5] C. Zander, and K. H., Drexhage, *Advances in Photochemistry* (Wiley, New York, 1995), Vol. 20, p. 59.
[6] C. B. Layne, W. H. Lowdermilk, and M. J. Weber, Phys. Rev. B **16**, 10 (1977).
[7] C. E. Mungan, M. I. Buchwald, B. C. Edwards, R. I. Epstein, and T. R. Gosnell, Phys. Rev. Lett. **78**, 1030 (1997).
[8] G. Lei, J. E. Anderson, M. I. Buchwald, B. C. Edwards, and R. I. Epstein, Spectral linewidths by absorption Voigt profiles in Yb^{3+}-doped fluorozirconate glasses, **57**, 7673 (1998).
[9] G. A. Niklasson and C. G. Granqvist in *Materials Science for Solar Energy Conversion Systems*, edited by C. G. Granqvist (Oxford, England; Pergamon, New York, 1991), p. 70.
[10] Laser Focus World **33**, 15 (1997).
[11] M. Razeghi, Opt. Photonics News **6**, 16 (1995).
[12] D. L. Griscom and E. J. Friebele, in *Fluoride Glass Fiber Optics*, edided by I. D. Aggarwal and G. Lu (Academic Boston, 1991), p. 307.
[13] P. T. Landsberg and G. Tonge, J. Appl. Phys. **51**, R1 (1980).
[14] L. Landau, J. Phys. (Moscow) **10**, 503 (1946).